

A study of the Inverse Gaussian Process with hazard rate functions-based drifts applied to degradation modelling

Indexed by:



Luis Alberto Rodríguez-Picón^{a,*}, Luis Carlos Méndez-González^a, Iván JC Pérez-Olguín^a,
Jesús Israel Hernández-Hernández^b

^aAutonomous University of Ciudad Juárez, Department Industrial Engineering and Manufacturing, Av. Plutarco Elías Calles 1210, Fovissste Chamizal, 32310 Ciudad Juárez, Chihuahua, México

^bAutonomous University of Ciudad Juárez, Department of Electrical and Computer Engineering, Av. Plutarco Elías Calles 1210, Fovissste Chamizal, 32310 Ciudad Juárez, Chihuahua, México


Highlights

- Flexible hazard rate functions are considered as drifts in the inverse Gaussian process.
- Degradation trajectories are characterized by the hazard rate functions-based drifts.
- Random effects are considered to individually characterize the degradation trajectories.
- Illustrative case studies are analysed to demonstrate the capability of proposed models.

Abstract

The stochastic modelling of degradation processes requires different characteristics to be considered, such that it is possible to capture all the possible information about a phenomenon under study. An important characteristic is what is known as the drift in some stochastic processes; specifically, the drift allows to obtain information about the growth degradation rate of the characteristic of interest. In some phenomenon's the growth rate cannot be considered as a constant parameter, which means that the rate may vary from trajectory to trajectory. Given this, it is important to study alternative strategies that allow to model this variation in the drift. In this paper, several hazard rate functions are integrated in the inverse Gaussian process to describe its drift in the aims of individually characterize degradation trajectories. The proposed modelling scheme is illustrated in two case studies, from which the best fitting model is selected via information criteria, a discussion of the flexibility of the proposed models is provided according to the obtained results.

Keywords

This is an open access article under the CC BY license (<https://creativecommons.org/licenses/by/4.0/>) 

inverse Gaussian process, hazard rate function, degradation rate, variable drift.

1. Introduction

One of the main approaches that has been considered in the last years for the reliability assessment of products and systems is based on degradation models. This modelling approach considers characterizing the degradation trajectory of a performance characteristic such that it is possible to extrapolate this trajectory to a critical level in the aims of obtaining pseudo failure times, from which a reliability assessment is performed. Degradation models based on stochastic processes have been proved to be an efficient alternative to model degradation processes as they consider the temporal uncertainty for the evolution of the degradation trajectory [41]. Furthermore, these models present different properties that are appealing to obtain reliability estimations [15, 21, 39].

Given different conditions of the products of interest and the experimental conditions, it results necessary to perform modifications in the modelling schemes of degradation process. For stochastic proc-

esses, these conditions can be incorporated considering random effects, which are defined by considering that one parameter of the stochastic process is a random variable. The inclusion of random effects is different for every stochastic process, e.g., for the gamma process, the scale parameter has been considered to integrate the random effects [12, 22, 30–32]. For the Wiener process, different schemes have been proposed in the literature to include random effects, these schemes consider that only the drift, only the diffusion of the process are random variables, or both are random variables [14, 28, 29, 33]. As for the inverse Gaussian (IG) process, different schemes have also been proposed that consider that only the drift or the shape are random parameters or both are random [5, 15, 18, 19, 34, 38]. The different schemes of inclusion of random effects in the different stochastic processes, generally obey to the visible characteristics of the degradation trajectories. If it is observed that there is a large variation of the degradation rates (variation between trajectories), then the drift

(*) Corresponding author.

E-mail addresses: L.A. Rodríguez-Picón (ORCID: 0000-0003-2951-2344): luis.picon@uacj.mx, L.C. Méndez-González (ORCID: 0000-0002-2533-0036): luis.mendez@uacj.mx, I.J.C. Pérez-Olguín (ORCID: 0000-0003-2445-0500): ivan.perez@uacj.mx, J.I. Hernández-Hernández (ORCID: 0000-0003-3807-565X): israel.hernandez@uacj.mx

of the stochastic process may be considered as a random variable to account for this variation. On the other hand, if it is observed that there is a large variation within the trajectories, *i.e.*, the large variation in the trajectory increments, then a parameter such as the diffusion in the Wiener process may be considered to account for this variation. Rodríguez-Picón [23] and Peng et al. [19] defined particular models for this scenario under the gamma and IG process. Finally, if a large variation between trajectories and within trajectories is noted, then multiple parameters of the stochastic process may be considered as random variables.

However, the behavior of the degradation trajectories may change over time, beyond the previously discussed scenarios based on variation, as they are continuously monitored. This means that the consideration of random effects in the modelling does not allow to describe the evolutive behavior of the degradation trajectories. Which means, that if a certain parameter of a stochastic process is considered to be random, this will not change the behavior of the trajectory, *i.e.*, if a trajectory is increasing then the inclusion of random effects will allow to account for the observed variation, but it will not account for the drift change of the trajectory. Peng et al. [20] presented an IG process with time-varying rates, they considered the mean function of the IG process to model monotonic degradation rates by considering the Weibull hazard rate function. When the parameters of the hazard rate are estimated then it is possible to note if the degradation rate is increasing, decreasing or constant. This is an important characteristic, as it is possible to determine the behavior of the trajectories' drift. On the other hand, probability distribution functions (PDF) that have flexible hazard rates have received great attention in the last years [2, 4, 7]. Several PDFs have been proposed in the literature to describe multiple hazard rate behaviors, such as increasing, decreasing, constant, bathtub shape, upside down bathtub shape and j-shape [10]. Hjorth [9] developed a distribution with increasing, decreasing, constant and bathtub-shaped hazard rate, the distribution is intuitive to detect these types of hazard rates based on the parameters of the distribution. SchÄbe [27] proposed lifetime distributions based on the truncation of PDFs which allowed to construct distributions with bathtub hazard rates. Xie and Lai [36] proposed a bathtub shaped failure rate distribution based on the addition of two Weibull distributions. Xie et al. [37] proposed a generalization of the Weibull distribution to describe bathtub failure rates, one parameter of the proposed distribution allows to define behaviors such as increasing, decreasing and bathtub shape. Lai et al. [11] proposed a distribution which is derived as a limiting case of the Beta Integrated Model and considered as a 3-parameter generalization of the Weibull distribution, this distribution also allows to describe bathtub hazard rates depending on the values of its parameters. Chen [6] also proposed a distribution that can describe bathtub hazard rates but with only two parameters. Dimitrakopoulou et al. [8] developed a three-parameter distribution that in addition to the increasing, decreasing and bathtub shapes also describes an upside-down bathtub shape. The Burr XII distribution has also been identified as a flexible model that can describe various forms of its hazard rate function [40]. Other distributions have been proposed in the literature that describe diverse shapes of the hazard rate functions. Although, as the number of parameters is high, the hazard rate function results in complex forms. Such is the case of the Beta-Weibull distribution [13], the exponentiated Weibull distribution [17], models based on the sum of hazard rate functions such as the exponentiated additive Weibull distribution [1], models that consist in the combination of different distributions to define new modelling capabilities [3, 25, 26].

Many manufactured products have complex characteristics and properties, which may result in an irregular degrading behavior of certain characteristic of interest. Based on this, the reliability modelling implies a complex task. In this paper, several flexible hazard rate functions, such as the Hjorth, Lai modified, and modified Xie models, are considered as the mean function of the IG process, this consideration allows to efficiently characterize the behavior of the degrada-

tion trajectories which may results in accurate reliability estimations. Furthermore, random effects are considered in the modelling in the aims of determining the behavior of each degradation trajectories according to the rules of every hazard rate function. As the hazard rate functions are directly related to the mean of the IG process, this increases the complexity of the model, thus an estimation scheme based on the MCMC Gibbs Sampling method is considered. The estimation procedure is implemented in the OpenBUGS software. The proposed models are compared with the IG-Weibull model proposed by Peng et al. [20] in two case studies. From which a discussion about the capability and flexibility of the modelling approach is provided.

The rest of this paper is organized as follows: In Section 2, the proposed modelling scheme based on the IG process and flexible hazard rates as drifts is presented and discussed. In Section 3, the estimation method based on a Bayesian approach is presented. In section 4, we present the considered case studies and the obtained results from the implementation of the proposed modelling approach. In Section 5, the discussion about the obtained results is presented, general insights are provided for the interpretation of the proposed modelling scheme. Finally, in Section 6 the conclusions are provided.

2. The inverse Gaussian process with hazard rate functions-based drifts

The IG process is a non-monotone stochastic process that models the behavior of a degradation process $(X(t); t > 0)$ over time (t) and has the property that the increments $\Delta X(t) = X(t + \Delta t) - X(t)$ follow an IG distribution $f_{IG}(\mu\Delta t, \eta\Delta t^2)$ and the increments $\Delta X(t)$ are independent. The parameter $\mu > 0$ represents the drift of the process, while $\eta > 0$ represents the shape parameter. Generally, this model is adequate to characterize the behavior of degradation process with additive and irreversible damages.

The PDF of $X(t)$ is defined based on the IG distribution as [19]:

$$f(X(t)|\mu, \eta, t) = \sqrt{\frac{\eta^2(t)}{2\pi X^2(t)}} \exp\left\{-\frac{\eta(X(t) - \mu(t))^2}{2\mu^2 X(t)}\right\}. \quad (1)$$

By considering that a degradation test is performed in a sample of n simultaneously used homogeneous devices of interest, with the consideration of (m) degradation measurements per device. Then the degradation measurements $X_i(t_j); i = 1, 2, \dots, n, j = 1, 2, \dots, m$, define degradation trajectories for each i with $j = 1, 2, \dots, m$. Furthermore, $X_i(t_j)$ follow an IG distribution as defined in (1). Thus, the degradation increments $\Delta X_i(t_j) = X_i(t_{j+1}) - X_i(t_j)$ follow an IG distribution as $\Delta X_i(t_j) \sim f_{IG}(\mu\Delta t_j, \eta\Delta t_j^2)$.

Based on these characteristics and considering that the parameter μ denotes the degradation rate. Then, it is possible to determine a particular parametric function to characterize the behavior of the degradation rate. One scenario result by considering that the rate is monotone [20], then it is adequate to consider the Weibull hazard rate as:

$$\mu(t) = \left(\frac{t}{\alpha_W}\right)^{\beta_W},$$

where, β_W and α_W are the shape and scale parameters of the Weibull distribution, respectively. Thus, the degradation rate depends on the estimated value of β_W , *i.e.*, when $0 < \beta_W < 1$ the rate is decreasing, when $\beta_W = 1$ the rate is constant and when $\beta_W > 1$ the rate is increasing. Although, these three scenarios are adequate for some degradation process, other hazard rate functions can be considered as the IG

drift to extend the flexibility of the model. For example, the Hjorth hazard rate is defined as:

$$h(t) = \delta t + \frac{\theta_H}{1 + \beta_H t} \quad (2)$$

Different behaviors can be described from this hazard rate [9], for example:

- When, $\delta = \beta_H = 0$; the rate is constant.
- When $\delta = 0$; the rate is decreasing.
- When $\delta \geq \theta_H \beta_H$; the rate is increasing.
- When $0 < \delta < \theta_H \beta_H$; the rate has a bathtub shape.

On the other hand, the hazard rate function defined by Dimitrakopoulou et al. (2007) is denoted as:

$$h(t) = \alpha_D \beta_D \lambda_D t^{\beta_D - 1} (1 + \lambda_D t^{\beta_D})^{\alpha_D - 1} \quad (3)$$

Again, different behaviors of the hazard rate can be described depending on the values of certain parameters, for example,

- When $\alpha_D = \beta_D = 1$; the rate is constant.
- When $\alpha_D > 1$ and $\beta_D \geq 1$; the rate is increasing.
- When $\alpha_D < 1$ and $\beta_D \leq 1$; the rate is decreasing
- When $\alpha_D \geq 1$ and $\beta_D < 1$, and $\alpha_D \beta_D > 1$; the rate has a bathtub shape.
- When $\alpha_D \leq 1$ and $\beta_D > 1$, and $\alpha_D \beta_D < 1$; the rate has a unimodal shape.

In addition to the previously discussed distributions, other hazard rate functions along with their respective proprieties are presented in Table 1. Furthermore, in Figure 1 different scenarios of the hazard rate are illustrated for every distribution under various values of the specific parameters. From this figure, it can be noted that the hazard rate models are flexible to describe a diverse amount of shapes.

The depicted behaviors of the hazard rates may be considered in the drift of the IG process in the aims of extend the flexibility of the

Table 1. Hazard rate functions for different distributions

Distribution	Hazard rate	Properties
Lai modified Weibull	$h(t) = \lambda_L (\beta_L + vt) t^{\beta_L - 1} \exp(vt)$	$\beta_L \geq 1$; increasing
		$0 < \beta_L < 1$; bathtub
Xie modified Weibull	$h(t) = \lambda_X \beta_X \left(\frac{t}{\alpha_X}\right)^{\beta_X - 1} \exp\left(\frac{t}{\alpha_X}\right)^{\beta_X}$	$\beta_X \geq 1$; increasing
		$0 < \beta_X < 1$; bathtub
SchÄbe	$h(t) = \frac{1}{\theta_S (\gamma + t / \theta_S)} + \frac{1}{\theta_S (\gamma - t / \theta_S)}$	$\gamma < 1$; bathtub
		$\gamma \geq 1$; increasing
Chen distribution	$h(t) = \lambda_C \beta_C t^{\beta_C - 1} \exp(t^{\beta_C})$	$\beta_C < 1$; Bathtub
		$\beta_C \geq 1$; increasing

stochastic process. Thus, it is considered that for the IG process the drift is defined as:

$$\mu(t) = \mu_h(t) = h(t) \quad (4)$$

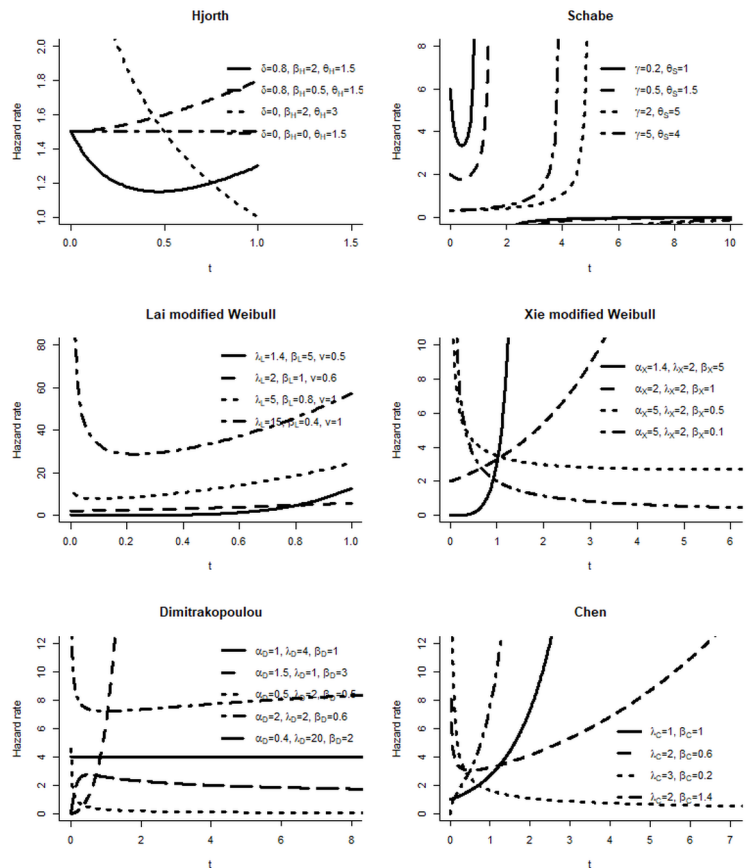


Fig. 1. Behaviors of the hazard rates of different distributions

Thus, the model for a degradation trajectory will have a PDF as described in (1) by considering the relation in (4) as $f(X(t)|\mu_h, \eta, t)$.

It should be noted that for some of the previously discussed PDFs in Table 1, the form of the hazard rate depends only on one parameter, then the estimation of this parameter may indicate the behavior of the IG drift. As in a degradation test, a total of n trajectories are expected to be observed, each one of this may have a specific behavior.

Thus, random effects may be considered in the hazard rate with the objective of estimating the hazard rate parameter that defines the behavior of the drift for every trajectory. For example, by considering the Xie modified Weibull model as the IG drift:

$$\mu_h(t) = \lambda_X \beta_X \left(\frac{t}{\alpha_X}\right)^{\beta_X - 1} \exp\left(\frac{t}{\alpha_X}\right)^{\beta_X}$$

Then β_X may be considered as a random effects parameteras β_{X_i} with PDF $\beta_{X_i} \sim f(\beta_{X_i} | a_{\beta_X}, b_{\beta_X})$. This parameter will be estimated for each trajectory $i = 1, 2, \dots, n$, which will allow to determine the shape of the drift individually. Then, the degradation model based on the IG process with the Xie modified Weibull hazard rate function-based drift and random effects has the following PDF:

$$f(X(t)|\eta, \lambda_X, \alpha_X, a_{\beta_X}, b_{\beta_X}, t) = \int_0^{\infty} f(X(t)|\lambda_X, \alpha_X, \beta_{X_i}, \eta, t) f(\beta_{X_i} | a_{\beta_X}, b_{\beta_X}) d\beta_{X_i} \quad (5)$$

The model in (5) can be modified for any hazard rate in Table 1 or the models described in (2) and (3). In general, the model for any hazard rate function $h(t) = \mu_h(t)$ with random effects results in:

$$f(X(t)|\eta, \mu_h(t), \theta_1, \theta_2, t) = \int_0^{\infty} f(X(t)|\mu_h(t), \eta, t) f(R_i|\theta_1, \theta_2) dR_i, \quad (6)$$

where, R_i represents a parameter from $\mu_h(t)$ that is selected to be random. On the other hand, θ_1 and θ_2 represent the parameters of the PDF that describes R_i .

3. The estimation of parameters

The model presented in (6) results in a quite complex form with no analytical expression. Indeed, the complexity of the model may increase depending on the selected hazard rate function for drift of the IG process. Despite the complexity of the model, it considers an important aspect that allows to adapt the drift of the process. On the other hand, it is of interest to estimate the parameters $(\eta, \mu_h(t), \theta_1, \theta_2)$ to assess the fitting of the model for specific degradation datasets. However, the classical estimation methods may result quite complicated to implement. Based on this, in this paper, a Bayesian estimation approach based on the Gibbs sampler and the Markov Chain Monte Carlo method is considered. This method has been found to be appropriate to estimate the parameters of complex functions given that it allows to sample from a desired distribution, such as the one in (6), to obtain consistent estimators of the parameters of interest [16]. Furthermore, the implementation of this method is relatively straightforward as there are several specialized open software's, which allow to implement complex function for estimation purposes. Specifically, the OpenBUGS software is considered to estimate the function in (6) under different scenarios of the hazard rate functions.

In general, non-informative prior distributions are considered for all the parameters of interest. Specifically, for η , the non-informative prior is a gamma distribution as $f_{\eta}(a_{\eta}, b_{\eta})$. As $\mu_h(t)$ may have different parametrizations, in general for all the possible combination of parameters, non-informative gamma distributions are considered. For example, for the Xie modified Weibull hazard rate, it is considered that the non-informative gamma distributions are defined as $f_{\lambda_X}(a_{\lambda_X}, b_{\lambda_X})$ and $f_{\alpha_X}(a_{\alpha_X}, b_{\alpha_X})$. Finally, for the selected random effects parameter R_i , the non-informative gamma distributions for its parameters are considered as $f_{\theta_1}(a_{\theta_1}, b_{\theta_1})$ and $f_{\theta_2}(a_{\theta_2}, b_{\theta_2})$.

On the other hand, considering that degradation measurements $\Delta X_i(t_j)$ have been observed for $i=1, 2, \dots, n$ and $j=1, 2, \dots, m$. Then, the likelihood function for the distribution of interest with random effects results in:

$$L(\Delta X_i(t_j)|\eta, \mu_h(t), \theta_1, \theta_2) = \prod_{i=1}^n \left\{ f(R_i|\theta_1, \theta_2) \prod_{j=1}^m f(\Delta X_i(t_j)|\mu_h(t), \eta) \right\}. \quad (7)$$

If random effects are not considered in the hazard rate for the IG process, then the parameters of interest are $(\eta, \mu_h(t))$, and the likelihood function is defined as:

$$L(\Delta X_i(t_j)|\eta, \mu_h(t)) = \prod_{i=1}^n \prod_{j=1}^m f(\Delta X_i(t_j)|\mu_h(t), \eta). \quad (8)$$

Considering the likelihood function in (7) and the previously described non-informative distributions. Then, assuming that the effects are independent, the posterior distribution with random effects is defined as:

$$p(\eta, \mu_h(t), \theta_1, \theta_2 | \Delta X_i(t_j)) \propto f_{\eta}(\eta) \times f_{\theta_1}(\theta_1) \times f_{\theta_2}(\theta_2) \times f_{\mu_h(t)}(\mu_h(t)) \times L(\Delta X_i(t_j)|\eta, \mu_h(t), \theta_1, \theta_2), \quad (9)$$

where, $f_{\mu_h(t)}(\mu_h(t))$ may represent a set of prior distributions, depending on the selected hazard rate function. While the posterior distribution for a model with no random effects is defined as:

$$p(\eta, \mu_h(t) | \Delta X_i(t_j)) \propto f_{\eta}(\eta) \times f_{\mu_h(t)}(\mu_h(t)) \times L(\Delta X_i(t_j)|\eta, \mu_h(t), \theta_1, \theta_2). \quad (10)$$

Again, $f_{\mu_h(t)}(\mu_h(t))$ represents a set of prior distributions depending on the selected hazard rate function. These posterior distributions are considered to implement the MCMC Gibbs sampler in OpenBUGS to obtain estimations of the parameters of interest. Specifically, a total of 70,000 iterations were considered for estimation purposes and 20,000 iterations for burn-in purposes. An example of the developed estimation code in OpenBUGS is presented as follows for the IG process with the Hjorth hazard rate and δ as a random parameter.

```

model {
  for (i in 1:N)
  {
    delta[i] ~ dgamma(shape, scale)
    for(j in 1:M-1)
    {
      x[i,j] ~ dinv.gauss(miu.u[i,j], eta.u[i,j])
      eta.u[i,j] <- eta.su * (pow(ts.u[i,j], 2))
      miu.u[i,j] <- ( (delta[i]*t[j+1]) + (theta/(1+(beta*t[j+1])) ) ) - (
        (delta[i]*t[j]) + (theta/(1+(beta*t[j])) ) ) )
      ts.u[i,j] <- ( t[j+1] - t[j] )
    }
  }
  shape ~ dgamma(1, 0.001)
  scale ~ dgamma(1, 0.001)
  theta ~ dgamma(0.1, 0.001)
  beta ~ dgamma(0.1, 0.001)
  eta.su ~ dgamma(0.1, 0.001)
}

```

4. Analysis of the considered case studies

Two cases studies are considered to illustrate the applicability of the proposed modelling approach. Several schemes of the discussed hazard rates are considered to describe the drift of the IG process. Furthermore, the parameters estimation approach based on the Bayesian method is implemented in OpenBUGS for all the models, and the performance for each scenario is compared based on the deviance information criterion (DIC), which is defined as:

$$DIC = -2 \log(L(X|\hat{\xi})) + 2p_{DIC},$$

where, $\hat{\xi}$ represents a set of parameters of interest, and p_{DIC} is an estimate of the effective number of parameters, which is obtained as the difference between the posterior mean deviance denoted as $\bar{D}(X|\hat{\xi}) = E(-2 \log(L(X|\hat{\xi}))|X)$ and the deviance at the posterior mean of $\hat{\xi}$, denoted as $D(X|\hat{\xi}) = -2 \log(L(X|\hat{\xi}))$.

$$p_{DIC} = \bar{D}(X|\hat{\xi}) - D(X|\hat{\xi})$$

For the two case studies, the next hazard rate functions were considered: Weibull (α_W, β_W) , Hjorth $(\delta, \theta_H, \beta_H)$, Dimitrakopoulou $(\alpha_D, \beta_D, \lambda_D)$, Lai modified Weibull $(\lambda_L, \beta_L, \nu)$, Xie modified Weibull $(\lambda_X, \beta_X, \alpha_X)$ and Chen (λ_C, β_C) . Random effects were considered for some of these hazard rate functions; in the case of the Weibull distribution the shape parameter β_{W_i} was considered to be random following a gamma distribution with shape parameter $a_{\beta_{W_i}}$ and scale parameter $b_{\beta_{W_i}}$. For the Hjorth rate, the parameter δ_i was considered to be random following a gamma distribution with shape parameter a_{δ_i} and scale parameter b_{δ_i} . While, for the Dimitrakopoulou rate the parameter α_{D_i} was considered to be random following a gamma distribution with shape parameter $a_{\alpha_{D_i}}$ and scale parameter $b_{\alpha_{D_i}}$. All the considered models are enlisted as follows:

1. The simple IG process denoted as $\Delta X_i(t_j) \sim IG(\mu \Delta t_j, \eta \Delta t_j^2)$.

2. The IG process with Weibull drift as:

$$\Delta X_i(t_j) \sim IG(\mu_h \Delta t_j, \eta \Delta t_j^2), \mu_h \Delta t_j = \left(\frac{t_{j+1}}{\alpha_W}\right)^{\beta_W} - \left(\frac{t_j}{\alpha_W}\right)^{\beta_W}.$$

3. The IG process with Weibull drift and random effects (IG-WRE) as:

$$\Delta X_i(t_j) \sim IG(\mu_h \Delta t_j, \eta \Delta t_j^2), \mu_h \Delta t_j = \left(\frac{t_{j+1}}{\alpha_W}\right)^{\beta_{W_i}} - \left(\frac{t_j}{\alpha_W}\right)^{\beta_{W_i}},$$

with a gamma distribution for $\beta_{W_i} \sim f(a_{\beta_{W_i}}, b_{\beta_{W_i}})$.

4. The IG process with Hjorth drift (IG-H) denoted as $\Delta X_i(t_j) \sim IG(\mu_h \Delta t_j, \eta \Delta t_j^2), \mu_h \Delta t_j = \delta t_{j+1} + \frac{\theta_H}{1 + \beta_H t_{j+1}} - \delta t_j + \frac{\theta_H}{1 + \beta_H t_j}$.

5. The IG process with Hjorth drift and random effects (IG-HRE) denoted as:

$$\Delta X_i(t_j) \sim IG(\mu_h \Delta t_j, \eta \Delta t_j^2), \mu_h \Delta t_j = \delta_i t_{j+1} + \frac{\theta_H}{1 + \beta_H t_{j+1}} - \delta_i t_j + \frac{\theta_H}{1 + \beta_H t_j},$$

with a gamma distribution for $\delta_i \sim f(a_{\delta_i}, b_{\delta_i})$.

6. The IG process with the Dimitrakopoulou drift (IG-DI) denoted as:

$$\Delta X_i(t_j) \sim IG(\mu_h \Delta t_j, \eta \Delta t_j^2), \mu_h \Delta t_j = \alpha_D \beta_D \lambda_D t_{j+1}^{\beta_D - 1} t_j^{\beta_D - 1} (1 + \lambda_D t_{j+1}^{\beta_D})^{\alpha_D - 1} - \alpha_D \beta_D \lambda_D t_j^{\beta_D - 1} t_{j-1}^{\beta_D - 1} (1 + \lambda_D t_j^{\beta_D})^{\alpha_D - 1}.$$

7. The IG process with the Dimitrakopoulou drift and random effects (IG-DI-RE) denoted as:

$$\Delta X_i(t_j) \sim IG(\mu_h \Delta t_j, \eta \Delta t_j^2), \mu_h \Delta t_j = \alpha_{D_i} \beta_D \lambda_D t_{j+1}^{\beta_D - 1} t_j^{\beta_D - 1} (1 + \lambda_D t_{j+1}^{\beta_D})^{\alpha_{D_i} - 1} - \alpha_{D_i} \beta_D \lambda_D t_j^{\beta_D - 1} t_{j-1}^{\beta_D - 1} (1 + \lambda_D t_j^{\beta_D})^{\alpha_{D_i} - 1}$$

with a gamma distribution for $\alpha_{D_i} \sim f(a_{\alpha_{D_i}}, b_{\alpha_{D_i}})$.

8. The IG process with the Lai modified Weibull drift (IG-LAI) denoted as:

$$\Delta X_i(t_j) \sim IG(\mu_h \Delta t_j, \eta \Delta t_j^2), \mu_h \Delta t_j = \lambda_L (\beta_L + \nu t_{j+1}) t_{j+1}^{\beta_L - 1} \exp(\nu t_{j+1}) - \lambda_L (\beta_L + \nu t_j) t_j^{\beta_L - 1} \exp(\nu t_j).$$

9. The IG process with the Xie modified Weibull drift (IG-XIE) denoted as:

$$\Delta X_i(t_j) \sim IG(\mu_h \Delta t_j, \eta \Delta t_j^2), \mu_h \Delta t_j = \lambda_X \beta_X \left(\frac{t_{j+1}}{\alpha_X}\right)^{\beta_X - 1} \exp\left(\frac{t_{j+1}}{\alpha_X}\right)^{\beta_X} - \lambda_X \beta_X \left(\frac{t_j}{\alpha_X}\right)^{\beta_X - 1} \exp\left(\frac{t_j}{\alpha_X}\right)^{\beta_X}.$$

10. The IG process with the Chen drift (IG-CH) denoted as:

$$\Delta X_i(t_j) \sim IG(\mu_h \Delta t_j, \eta \Delta t_j^2), \mu_h \Delta t_j = \lambda_C \beta_C t_{j+1}^{\beta_C - 1} \exp(t_{j+1}^{\beta_C - 1}) - \lambda_C \beta_C t_j^{\beta_C - 1} \exp(t_j^{\beta_C - 1}).$$

4.1. Fatigue crack propagation dataset

The first case study consists of the propagation of a fracture in a terminal presented by Rodríguez-Picón et al. [24]. The authors performed a degradation test based on a vibration profile, that ranges

from 0.1 hundred thousand cycles to 0.9 hundred thousand cycles, to study the propagation of a fracture as a measure of the cracks' length increase in millimeters (mm). Degradation measurements $X_i(t_j)$ were obtained for $i = 1, 2, \dots, 10$ devices at $j = 0, 1, \dots, 10$. From these measurements the cumulative degradation trajectories can be characterized as illustrated in Figure 2. As reported by Rodríguez-Picón et al. [24], the critical level of degradation is determined to be 0.4 mm. The crack of two devices reached this critical level at the end of the degradation test. It can be noted from Figure 2, that there is a great variation in the behavior of the degradation trajectories, which enables to consider different approaches to model these trajectories. The ten models previously enlisted were implemented to this degradation dataset. For this, the Bayesian estimation approach described in Section 3 was considered. In Table 1, the estimations of all the parameters for all the scenarios are presented. Furthermore, the standard deviation (SD) and Monte Carlo (MC) error are provided along with the $P_{0.025}, P_{0.5}, P_{0.975}$ percentiles. It can be noted that for the models with random effects, the estimations of the parameter defined as random are provided according to the number of trajectories.

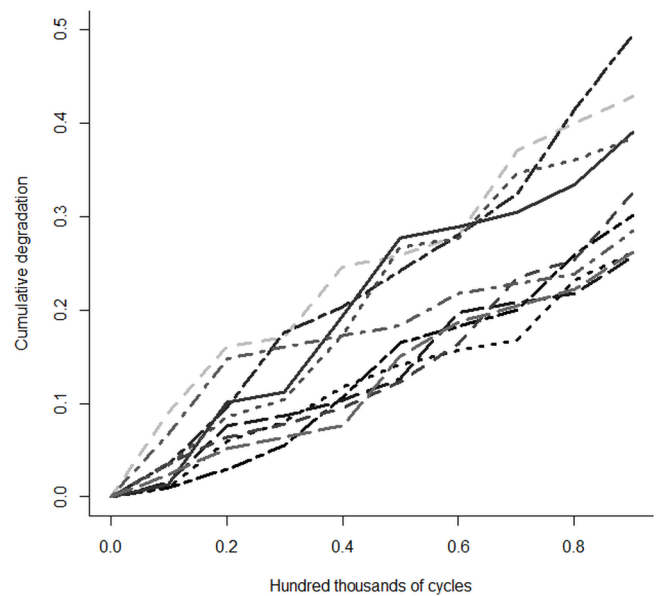


Fig. 2. Crack propagation trajectories for the first case study [24]

In Table 2, the DIC is presented for the ten considered modelling schemes. Along with the DIC the ranking for each model is presented by considering that the model with the lowest value of the DIC is considered to be the best fitting model. It can be noted that the model with the lowest DIC is the IG with the Hjorth hazard rate-based drift and δ_i as a random effects parameter with a value of -2178. The second-best model is the IG with Hjorth hazard rate-based drift and no random effects with a DIC value of -593.2. There is a big difference between the DICs values of these two models, which mean that the IG-HRE is definitely the best fitting model. Furthermore, the model with the poorest performance is the IG with Chen hazard rate-based drift. It can be also noted that the simple IG model and the IG with Weibull hazard rate-based drift proposed by Peng et al. [20] are ranked in 6th and 7th place respectively, which denotes that the currently proposed models in the literature do not characterize the degradation trajectories efficiently.

4.2. Aluminum alloy crack growth study

The second case study was presented by Wu and Ni [35] and consisted in a degradation test performed to a batch of 2024-T351 aluminum alloy specimens. The authors considered a dynamic testing to perform vibration load cycles from 10,000 to 40,000 to the speci-

Table 1. Obtained estimations for the first case study and all the considered models

Model	Parameter	Mean	SD	MC error	$P_{0.025}$	$P_{0.5}$	$P_{0.975}$
IG	μ	6.025	0.8943	2.99E-03	4.396	5.985	7.901
	η	0.3855	0.03397	1.21E-04	0.3275	0.3825	0.4609
IG-W	β_W	0.9753	0.09859	6.38E-04	0.7668	0.9799	1.155
	α_W	2.718	0.3697	0.00248	2.078	2.688	3.522
	η	5.955	0.8824	0.00323	4.363	5.91	7.8
IG-W-RE	β_{W1}	0.9749	0.1144	0.00485	0.7276	0.9818	1.18
	β_{W2}	0.9597	0.1078	0.00463	0.723	0.9676	1.148
	β_{W3}	0.9749	0.1141	0.00483	0.7285	0.9819	1.178
	β_{W4}	0.9738	0.1134	0.00481	0.7265	0.9807	1.175
	β_{W5}	0.9646	0.1107	0.00473	0.7233	0.9715	1.16
	β_{W6}	0.9675	0.1118	0.00476	0.7245	0.9744	1.165
	β_{W7}	0.9721	0.1122	0.00478	0.7281	0.9792	1.171
	β_{W8}	0.9666	0.1113	0.00474	0.7243	0.974	1.162
	β_{W9}	0.9657	0.1091	0.00468	0.726	0.973	1.156
	β_{W10}	0.974	0.1133	0.00481	0.7272	0.9807	1.176
	α_W	2.733	0.385	0.0126	2.086	2.697	3.592
	η	5.964	0.8963	0.00688	4.336	5.919	7.844
	$a_{\beta_{W_i}}$	1326	804.2	45.98	234.4	1142	3594
	$b_{\beta_{W_i}}$	1271	744.6	42.49	227.9	1093	2851
IG-H	β_H	0.2022	0.6773	0.02257	7.77E-20	1.92E-04	2.423
	δ	0.3975	0.05178	0.001674	0.3289	0.3884	0.5315
	η	5.905	0.8836	0.006772	4.318	5.86	7.736
	θ_H	47.31	210.6	5.938	2.94E-11	0.05462	512.7
IG-H-RE	β_H	58.22	239.9	6.71	5.29E-13	0.01073	635.9
	δ_1	0.3916	0.05005	0.003141	0.3192	0.3847	0.5158
	δ_2	0.396	0.04985	0.003165	0.3242	0.3883	0.5205
	δ_3	0.3901	0.04984	0.003125	0.317	0.3832	0.5128
	δ_4	0.3899	0.04996	0.003151	0.3162	0.3829	0.5098
	δ_5	0.3982	0.04991	0.003183	0.3264	0.3906	0.5192
	δ_6	0.3948	0.04994	0.003172	0.3221	0.3872	0.5186
	δ_7	0.3925	0.0498	0.003152	0.32	0.3849	0.5134
	δ_8	0.3944	0.04962	0.003143	0.3217	0.3874	0.5171
	δ_9	0.3909	0.04982	0.00315	0.3175	0.3839	0.5118
	δ_{10}	0.3902	0.04976	0.003126	0.3177	0.3834	0.5104
	η	5.924	0.8847	0.006718	4.312	5.877	7.772
	a_{δ_i}	1465	702.8	58.21	434.9	1354	3097
	b_{δ_i}	569.4	264.1	21.81	165.2	529.5	1152
θ_H	11.89	47.76	1.778	1.06E-15	0.002033	146.2	
IG-DI	α_D	1.262	0.9819	0.09716	3.39E-01	0.943	4.07
	β_D	2.014	0.1418	0.009797	1.74E+00	2.015	2.292
	η	5.768	0.864	0.01476	4.20E+00	5.731	7.537
	λ_D	0.2568	0.1835	0.01757	4.52E-02	0.2105	0.7503

IG-DI-RE	α_{D1}	0.9211	0.3041	0.02462	0.3861	0.8961	1.556
	α_{D2}	0.928	0.3056	0.02475	0.39	0.9007	1.556
	α_{D3}	0.918	0.3034	0.02457	0.3819	0.8953	1.552
	α_{D4}	0.9173	0.3041	0.02462	0.3822	0.8936	1.548
	α_{D5}	0.9333	0.3066	0.02484	0.3942	0.9076	1.569
	α_{D6}	0.9257	0.3057	0.02475	0.3881	0.8992	1.561
	α_{D7}	0.9228	0.3038	0.0246	0.3884	0.8991	1.552
	α_{D8}	0.9251	0.3058	0.02477	0.3857	0.8994	1.562
	α_{D9}	0.9187	0.3037	0.02458	0.3829	0.8941	1.552
	α_{D10}	0.9174	0.3031	0.02455	0.3805	0.8935	1.541
	β_D	2.017	0.117	0.005515	1.777	2.018	2.249
	η	5.823	0.886	0.008678	4.225	5.782	7.686
	λ_D	0.2547	0.1254	0.009851	0.1177	0.222	0.613
	$a_{\alpha_{Di}}$	898.4	404.9	33.57	252.2	833.2	1762
$b_{\alpha_{Di}}$	776.9	328.1	27.2	193.8	775.3	1435	
IG-LAI	β_L	1.958	0.1308	0.003648	1.635	1.974	2.164
	η	5.818	0.8699	0.006059	4.24	5.767	7.634
	λ_L	0.1888	0.0259	7.46E-04	0.1331	0.1886	0.2406
	ν	0.04278	0.1004	0.004233	1.73E-16	3.18E-04	0.376
IG-XIE	α_X	21.8	36.71	2.46	1.671	7.568	133.7
	β_X	1.947	0.1334	0.005281	1.633	1.963	2.16
	η	5.806	0.8699	0.006748	4.243	5.761	7.657
	λ_X	4.353	8.294	0.5436	0.2357	1.411	29.1
IG-CH	β_C	1.425	0.176	0.002345	1.105	1.421	1.774
	η	5.148	0.7725	0.005844	3.737	5.113	6.754
	λ_C	0.1388	0.02412	3.89E-04	0.1065	0.1337	0.2015

mens. They recorded the cracks length increments of the specimens until a total fracture was observed. Thus, degradation measurements $X_i(t_j)$ were obtained for $i=1,2,\dots,30$ and $j=0,1,2,3,4$ with $(t_0=0, t_1=1, t_2=2, t_3=3, t_4=4) \times 10^4$ cycles. From these measurements, the trajectories are characterized as illustrated in Figure 3. From Figure 3, it can be noted that some of the trajectories have a higher degradation rate, specifically the ones that are on top. While, other trajectories have a lower degradation rate, specifically the ones that are on the bottom. These differences in degradation rate allows to consider that the degradation rate needs to be considered as a flexible function. Furthermore, Wu and Ni [35] considered a stochastic fatigue

crack growth model based on the Paris-Erdogan law, which does not consider the flexibility of the degradation rates. In the aims demonstrate the applicability of the proposed modelling scheme, the ten proposed models were fitted to the dataset by considering the Bayesian estimation procedure. The obtained results are presented in Table 3, where the estimations for the corresponding parameters are presented in the *mean* column, SD, MC error and the percentiles $p_{0.025}$, $p_{0.5}$, $p_{0.975}$ are also provided.

Table 2. DIC values and rankings for the models estimated in the first case study

Model	DIC	Ranking
IG	-438.1	6
IG-W	-436	7
IG-W-RE	-435.7	9
IG-H	-593.2	2
IG-H-RE	-2178	1
IG-DI	-464.8	3
IG-DI-RE	-440.1	5
IG-LAI	-435.9	8
IG-XIE	-440.3	4
IG-CH	-425.1	10

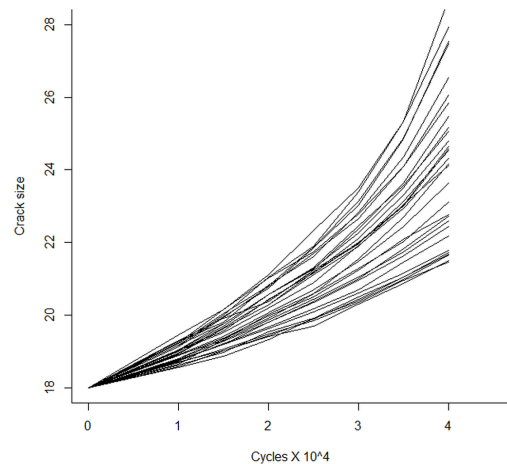


Fig. 3. Crack propagation trajectories for the second case study

In Table 4, the obtained DIC values for all the fitted models are provided. Again, the best fitting model is considered as the one with the lowest DIC value. For this dataset, the IG model with the Hjorth hazard rate-based drift and random effects has the lowest DIC value as -2620. The second-best fitting model, as in the case of the first case study, is the IG model with Hjorth hazard rate-based drift and without random effects with a DIC value of -2143. It can also be noted that the two models with the highest DIC values are the simple IG and the IG model with Weibull hazard rate-based drift, which denotes that these models have the poorest performance.

5. Discussion

The best fitting models for the two case studies can be further analyzed according to the considered hazard rate functions. For the first case study, it was found that the Hjorth hazard rate-based drift with random effects is the best fitting model for the degradation trajectories. As this model considers the δ_i parameter as random, then this parameter was estimated for each trajectory as can be noted in Table 1. Furthermore, the shape of the drift can be further analyzed by considering the properties discussed in Section 2. Particularly, it was

Table 3. Estimated parameters for the second case study

Model	Parameter	Mean	SD	MC error	$P_{0.025}$	$P_{0.5}$	$P_{0.975}$
IG	η	15.22	1.607	0.01124	12.24	15.15	18.54
	μ	1.754	0.06278	4.52E-04	1.636	1.752	1.882
IG-W	β_W	1.714	0.0682	0.001694	1.578	1.714	1.849
	α_W	1.443	0.0604	0.001518	1.318	1.445	1.555
	η	23.98	2.517	0.0198	19.34	23.88	29.22
IG-W-RE	β_{W1}	1.295	0.051	6.42E-04	1.201	1.293	1.403
	β_{W2}	1.468	0.06085	8.32E-04	1.356	1.465	1.596
	β_{W3}	1.879	0.09107	0.001349	1.715	1.874	2.072
	β_{W4}	1.91	0.09147	0.001434	1.746	1.904	2.104
	β_{W5}	1.777	0.08171	0.001247	1.628	1.774	1.948
	β_{W6}	1.729	0.07836	0.001123	1.587	1.726	1.894
	β_{W7}	1.931	0.0904	0.0013	1.766	1.927	2.124
	β_{W8}	1.275	0.04971	6.61E-04	1.183	1.273	1.379
	β_{W9}	2.062	0.101	0.001662	1.877	2.057	2.274
	β_{W10}	1.221	0.04604	5.91E-04	1.137	1.219	1.317
	β_{W11}	1.406	0.05727	7.69E-04	1.301	1.403	1.526
	β_{W12}	2.04	0.09898	0.001649	1.861	2.035	2.249
	β_{W13}	1.719	0.07708	0.00104	1.581	1.715	1.882
	β_{W14}	1.677	0.07338	0.001023	1.545	1.673	1.833
	β_{W15}	1.294	0.05129	6.73E-04	1.2	1.292	1.403
	β_{W16}	1.807	0.08416	0.001222	1.651	1.803	1.983
	β_{W17}	1.734	0.07921	0.001066	1.589	1.731	1.901
	β_{W18}	1.68	0.0763	9.88E-04	1.54	1.677	1.841
	β_{W19}	1.457	0.06127	7.20E-04	1.346	1.454	1.586
	β_{W20}	1.204	0.0456	6.26E-04	1.12	1.202	1.299
	β_{W21}	1.691	0.07548	0.001052	1.554	1.688	1.851
	β_{W22}	1.269	0.04972	6.46E-04	1.179	1.267	1.373
	β_{W23}	1.603	0.0694	9.15E-04	1.477	1.6	1.748
	β_{W24}	1.361	0.05412	7.33E-04	1.262	1.359	1.474
	β_{W25}	1.772	0.08104	0.001149	1.626	1.769	1.943
	β_{W26}	2.033	0.09774	0.001615	1.856	2.028	2.241
	β_{W27}	1.531	0.0653	9.37E-04	1.411	1.528	1.666
	β_{W28}	1.417	0.05884	7.97E-04	1.31	1.414	1.541
	β_{W29}	1.846	0.08622	0.001228	1.691	1.841	2.028
	β_{W30}	2.136	0.1045	0.001743	1.949	2.13	2.359
α_W	1.409	0.03044	8.03E-04	1.349	1.41	1.468	
η	97.52	11.23	0.1063	76.95	97.05	121.1	
$a_{\beta_{W_i}}$	22.57	6.175	0.401	12.23	22.08	36.81	
$b_{\beta_{W_i}}$	36.96	9.935	0.6449	20.29	36.24	60.06	

IG-H	β_H	0.05466	0.05342	0.002552	0.01524	0.03533	0.2033
	δ	9.88E+00	4.61E+00	0.2338	3.305	9.188	18.73
	η	23.69	2.514	0.01769	19.02	23.6	28.88
	θ_H	373.5	349.1	17.72	17.18	248.9	1160
IG-H-RE	β_H	0.03862	0.009497	4.74E-04	0.02584	0.03643	0.06454
	δ_1	6.112	0.9846	0.04914	4.084	6.164	8.043
	δ_2	6.296	0.9859	0.04913	4.269	6.347	8.224
	δ_3	7.032	0.9992	0.04923	4.994	7.082	8.97
	δ_4	7.059	0.9991	0.0492	5.027	7.107	8.996
	δ_5	6.792	0.9937	0.04917	4.756	6.843	8.722
	δ_6	6.737	0.9928	0.04918	4.708	6.787	8.669
	δ_7	7.055	0.9992	0.0492	5.019	7.106	8.992
	δ_8	6.079	0.9847	0.04916	4.05	6.128	8.006
	δ_9	7.328	1.005	0.04925	5.287	7.373	9.269
	δ_{10}	5.946	0.9836	0.04915	3.923	5.996	7.873
	δ_{11}	6.264	0.9857	0.04913	4.239	6.315	8.192
	δ_{12}	7.292	1.004	0.04923	5.251	7.339	9.235
	δ_{13}	6.714	0.9924	0.04917	4.684	6.765	8.648
	δ_{14}	6.596	0.9892	0.0491	4.57	6.647	8.519
	δ_{15}	6.047	0.984	0.04916	4.023	6.098	7.971
	δ_{16}	6.865	0.9952	0.04918	4.832	6.916	8.797
	δ_{17}	6.708	0.9918	0.04914	4.677	6.756	8.63
	δ_{18}	6.684	0.9922	0.04918	4.648	6.735	8.611
	δ_{19}	6.336	0.9865	0.04914	4.307	6.388	8.261
	δ_{20}	6.016	0.9846	0.04917	3.989	6.065	7.945
	δ_{21}	6.618	0.9898	0.04912	4.587	6.669	8.545
	δ_{22}	6.115	0.9853	0.04917	4.087	6.164	8.04
	δ_{23}	6.486	0.9879	0.04912	4.458	6.54	8.41
	δ_{24}	6.203	0.9847	0.04911	4.178	6.254	8.133
	δ_{25}	6.798	0.9938	0.04917	4.767	6.849	8.725
	δ_{26}	7.279	1.004	0.04922	5.236	7.326	9.217
	δ_{27}	6.423	0.9869	0.04911	4.398	6.474	8.351
	δ_{28}	6.234	0.9853	0.04914	4.21	6.285	8.155
	δ_{29}	6.932	0.9956	0.04913	4.898	6.982	8.857
	δ_{30}	7.492	1.009	0.04926	5.45	7.536	9.437
	η	68.31	7.969	0.04693	53.62	68.01	84.69
a_{δ_i}	34.93	10.29	0.4762	17.87	33.61	57.58	
b_{δ_i}	235	87.79	4.222	96.04	218.4	431.1	
θ_H	165.6	58.88	2.973	61.45	164.9	293.2	
IG-DI	δ_{12}	3.283	1.518	0.127	1.245	2.934	7.177
	δ_{13}	1.301	0.3699	0.0309	0.83	1.224	2.241
	δ_{14}	24.49	2.61	0.02612	19.65	24.42	29.85
	δ_{15}	0.24	0.04577	0.003546	0.139	0.242	0.3227

IG-DI-RE	α_1	2.698	0.3977	0.03304	2.084	2.684	3.724
	α_2	2.853	0.4161	0.03454	2.206	2.837	3.922
	α_3	3.236	0.4645	0.03844	2.51	3.222	4.431
	α_4	3.248	0.4662	0.0386	2.521	3.232	4.45
	α_5	3.127	0.451	0.03737	2.426	3.112	4.29
	α_6	3.094	0.4471	0.03706	2.398	3.077	4.251
	α_7	3.246	0.4651	0.03851	2.525	3.23	4.447
	α_8	2.679	0.3948	0.0328	2.066	2.665	3.698
	α_9	3.36	0.4799	0.0397	2.61	3.344	4.599
	α_{10}	2.603	0.3826	0.03182	2.009	2.589	3.596
	α_{11}	2.809	0.4123	0.03423	2.171	2.793	3.88
	α_{12}	3.343	0.4776	0.03953	2.599	3.326	4.573
	α_{13}	3.082	0.4457	0.03695	2.386	3.065	4.227
	α_{14}	3.031	0.4383	0.03634	2.349	3.016	4.158
	α_{15}	2.689	0.3956	0.03287	2.08	2.673	3.716
	α_{16}	3.159	0.4551	0.0377	2.447	3.143	4.33
	α_{17}	3.086	0.4455	0.03693	2.393	3.072	4.23
	α_{18}	3.062	0.4436	0.03678	2.374	3.045	4.206
	α_{19}	2.86	0.4184	0.03473	2.215	2.845	3.94
	α_{20}	2.614	0.3868	0.03215	2.014	2.6	3.615
	α_{21}	3.045	0.4396	0.03644	2.358	3.03	4.174
	α_{22}	2.684	0.3963	0.03292	2.073	2.669	3.712
	α_{23}	2.971	0.4318	0.03582	2.305	2.955	4.091
	α_{24}	2.764	0.4066	0.03376	2.133	2.75	3.815
	α_{25}	3.126	0.4511	0.03737	2.426	3.11	4.292
	α_{26}	3.339	0.4769	0.03947	2.596	3.321	4.564
	α_{27}	2.919	0.4257	0.03533	2.257	2.903	4.018
	α_{28}	2.808	0.4113	0.03416	2.173	2.795	3.873
	α_{29}	3.189	0.4582	0.03794	2.481	3.175	4.367
	α_{30}	3.421	0.4879	0.04035	2.656	3.406	4.672
β_D	1.177	0.09492	0.007873	1.001	1.168	1.356	
η	129.9	15.08	0.1666	101.8	129.4	161.1	
λ_D	0.2674	0.0197	0.001538	0.2236	0.2681	0.3023	
$a_{\alpha_{Di}}$	58.31	15.2	1.204	35.45	56.24	91.14	
$b_{\alpha_{Di}}$	173.1	42.37	3.332	97.82	171.9	260.1	
IG-LAI	β_L	1.993	0.5088	0.04204	1.109	1.901	2.771
	η	24.55	2.645	0.04322	19.68	24.43	30.05
	λ_L	0.4303	0.26	0.0208	0.1742	0.3674	1.138
	ν	0.1285	0.0846	0.00691	3.6E-10	0.1525	0.2535
IG-XIE	α_X	5.257	1.727	0.1686	2.344	5.165	9.693
	β_X	1.686	0.4612	0.0441	0.8857	1.702	2.556
	η	25.15	2.619	0.03849	20.24	25.05	30.5
	λ_X	3.01	1.588	0.1529	1.777	2.549	8.125
IG-CH	β_C	0.6611	0.02709	0.001784	0.5951	0.664	0.7058
	η	24.46	2.627	0.02276	19.63	24.38	29.93
	λ_C	1.677	0.4554	0.0312	1.119	1.573	2.998

Table 4. DIC values and rankings for the fitted models of the second case study.

Model	DIC	Ranking
IG	141.9	10
IG-W	61.29	9
IG-W-RE	-163.8	5
IG-H	-2143	2
IG-H-RE	-2620	1
IG-DI	-235.7	4
IG-DI-RE	-252.8	3
IG-LAI	21.69	7
IG-XIE	15.14	6
IG-CH	53.76	8

Table 5. Detecting the rate shape for the trajectories of the second case study

Trajectory (<i>i</i>)	δ_i	$\theta_H \beta_H$	Shape of rate
1	6.112	6.395	Bathtub
2	6.296	6.395	Bathtub
3	7.032	6.395	Increasing
4	7.059	6.395	Increasing
5	6.792	6.395	Increasing
6	6.737	6.395	Increasing
7	7.055	6.395	Increasing
8	6.079	6.395	Bathtub
9	7.328	6.395	Increasing
10	5.946	6.395	Bathtub
11	6.264	6.395	Bathtub
12	7.292	6.395	Increasing
13	6.714	6.395	Increasing
14	6.596	6.395	Increasing
15	6.047	6.395	Bathtub
16	6.865	6.395	Increasing
17	6.708	6.395	Increasing
18	6.684	6.395	Increasing
19	6.336	6.395	Bathtub
20	6.016	6.395	Bathtub
21	6.618	6.395	Increasing
22	6.115	6.395	Bathtub
23	6.486	6.395	Increasing
24	6.203	6.395	Bathtub
25	6.798	6.395	Increasing
26	7.279	6.395	Increasing
27	6.423	6.395	Increasing
28	6.234	6.395	Bathtub
29	6.932	6.395	Increasing
30	7.492	6.395	Increasing

denoted that if $0 < \delta_i < \theta_H \beta_H$, then the rate has a bathtub shape. By considering from Table 2 that $\theta_H = 11.89$, $\beta_H = 58.22$ and the individual values of $\delta_i, i = 1, 2, \dots, 10$, it can be noted that $0 < \delta_i < \theta_H \beta_H$

results as $0 < \delta_i < 692.2358 \forall i$. Thus, for this particular case study, the best fitting model detects that all the trajectories have a bathtub rate.

On the other hand, from the obtained results of the second case study it was found that the best fitting model is also the Hjorth hazard rate-based drift with random effects is the best model. From the Table 3, it can be noted that the values of δ_i vary from trajectory to trajectory. Again, the estimated parameters allow to analyze the behaviors of the trajectory' rates individually. Besides the case when $0 < \delta_i < \theta_H \beta_H$, which denotes a bathtub shape rate, it is known that when $\delta_i \geq \theta_H \beta_H$ then the degradation rate is increasing. These two properties can be analyzed for this case study by considering the estimations from Table 3. In Table 5, the product $\theta_H \beta_H$ is compared with δ_i for $i = 1, 2, \dots, 30$ in the aims of detecting the individual degradation rates.

It can be noted from Table 5, that $0 < \delta_i < 6.395$ for $i = 1, 2, 8, 10, 11, 15, 19, 20, 22, 24, 28$, which means that these trajectories have a bathtub rate. While, for the rest of the trajectories it can be noted that $\delta_i \geq 6.395$, which denotes that these trajectories have an increasing rate. These results are illustrated in Figure 4, where the red dashed lines represent the trajectories with bathtub rates and the continuous black lines denote the trajectories with increasing rate. It can be noted that the increasing rate trajectories are well identified as the degradation rate is continuously growing compared with the trajectories with bathtub rates.

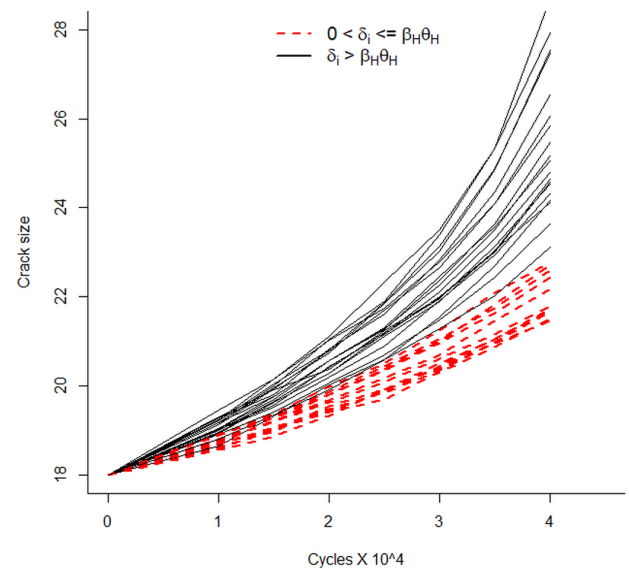


Fig. 4. Illustration of the bathtub and increasing rates of the second case study

6. Conclusion

The degradation rate is an important aspect to be considered when modelling the degradation process of a characteristic of interest. As this aspect may not be constant given the homogenous characteristics of the specimen under test or the environmental conditions. In this paper, a modelling approach was considered based on the inclusion of different hazard rate functions in the drift of the IG process. This inclusion allows to efficiently describe the behaviour of the degradation rates, as the hazard rate functions have flexible behaviours that can be characterized according to certain values of its parameters. From the analysed case studies, it was found that the best fitting models were those considering the Hjorth hazard rate as the drift in the IG process besides the consideration of δ_i as a random effects parameter. In first instance, there was a clear difference of the DIC values of the different models and the IG-H-RE model. Indicating a clear advantage over the simple IG process and the IG with Weibull rate model proposed by

Peng et al. [20]. Furthermore, the Hjorth model with random effects allowed to identify the behaviour of each trajectory individually. For the first case study, it was found that all the trajectories have bathtub rates, while for the second case study it was found that a set of trajectories have an increasing rate, and the other set of trajectories have a bathtub rate. The degradation rates of the individually identified trajectories was illustrated in Figure 4. This modelling approach presents the advantage of individually characterize the degradation trajectories, which may present important advantages for the reliability assessment of products and systems. There are several aspects that can be extended for further research. In first instance, other approaches with

multiple random effects can be studied for several hazard rate functions. This may allow to improve the characterization of the degradation trajectories. Although, this implies to deal with complex models that may require major computational resources. Furthermore, other sources of uncertainty may be considered in the IG process such as measurement errors. Finally, other hazard rate functions can be considered to describe the drift of the IG process. Although, other PDFs have been proposed in the literature that can describe a wide range of hazard rate behaviours, the parametric form of the hazard rates may be complex with non-closed terms which would result in a complex model to be estimated.

References

- Ahmad A E B A, Ghazal M G M. Exponentiated additive Weibull distribution. *Reliability Engineering & System Safety* 2020; 193: 106663, <https://doi.org/10.1016/J.RESS.2019.106663>.
- Ahsan S, Lemma T A, Gebremariam M A. Reliability analysis of gas turbine engine by means of bathtub-shaped failure rate distribution. *Process Safety Progress* 2020; 39(S1): e12115, <https://doi.org/10.1002/PRS.12115>.
- Ali S, Ali S, Shah I, Khajavi A N. Reliability Analysis for Electronic Devices Using Beta Generalized Weibull Distribution. *Iranian Journal of Science and Technology, Transactions A: Science* 2019 43:5 2019; 43(5): 2501–2514, <https://doi.org/10.1007/S40995-019-00730-4>.
- Andrzejczak K, Selech J. Generalised gamma distribution in the corrective maintenance prediction of homogeneous vehicles. *Lecture Notes in Networks and Systems* 2019; 68: 519–529, https://doi.org/10.1007/978-3-030-12450-2_50/COVER/.
- Chen N, Ye Z S, Xiang Y, Zhang L. Condition-based maintenance using the inverse Gaussian degradation model. *European Journal of Operational Research* 2015; 243(1): 190–199, <https://doi.org/10.1016/J.EJOR.2014.11.029>.
- Chen Z. A new two-parameter lifetime distribution with bathtub shape or increasing failure rate function. *Statistics & Probability Letters* 2000; 49(2): 155–161, [https://doi.org/10.1016/S0167-7152\(00\)00044-4](https://doi.org/10.1016/S0167-7152(00)00044-4).
- Chiodo E, Mazzanti G. The Decreasing Hazard Rate Phenomenon: A Review of Different Models, with a Discussion of the Rationale behind Their Choice. *Electronics* 2021, Vol. 10, Page 2553 2021; 10(20): 2553, <https://doi.org/10.3390/ELECTRONICS10202553>.
- Dimitrakopoulou T, Adamidis K, Loukas S. A lifetime distribution with an upside-down bathtub-shaped hazard function. *IEEE Transactions on Reliability* 2007; 56(2): 308–311, <https://doi.org/10.1109/TR.2007.895304>.
- Hjorth U. A Reliability Distribution with Increasing, Decreasing, Constant and Bathtub-Shaped Failure Rates. *Technometrics* 1980; 22(1): 99, <https://doi.org/10.2307/1268388>.
- Kayid M. Some new results on bathtub-shaped hazard rate models. *Mathematical Biosciences and Engineering* 2022 2:1239 2022; 19(2): 1239–1250, <https://doi.org/10.3934/MBE.2022057>.
- Lai C D, Xie M, Murthy D N P. A modified Weibull distribution. *IEEE Transactions on Reliability* 2003; 52(1): 33–37, <https://doi.org/10.1109/TR.2002.805788>.
- Lawless J, Crowder M. Covariates and Random Effects in a Gamma Process Model with Application to Degradation and Failure. *Lifetime Data Analysis* 2004; 10(3): 213–227, <https://doi.org/10.1023/B:LIDA.0000036389.14073.dd>.
- Lee C, Famoye F, Olumolade O. Beta-Weibull Distribution: Some Properties and Applications to Censored Data. *Journal of Modern Applied Statistical Methods* 2007; 6(1): 17, <https://doi.org/10.22237/jmasm/1177992960>.
- Li C, Hao H. Degradation Data Analysis Using Wiener Process and MCMC Approach. *Engineering Letters* 2017; 25(3): 234–238.
- Liu D, Wang S, Tomovic M M. Degradation modeling method for rotary lip seal based on failure mechanism analysis and stochastic process. *Eksplatacja i Niezawodność – Maintenance and Reliability* 2020; 22(3): 381–390, <https://doi.org/10.17531/EIN.2020.3.1>.
- Luengo D, Martino L, Bugallo M et al. A survey of Monte Carlo methods for parameter estimation. *EURASIP Journal on Advances in Signal Processing* 2020 2020:1 2020; 2020(1): 1–62, <https://doi.org/10.1186/S13634-020-00675-6>.
- Mudholkar G S, Srivastava D K. Exponentiated Weibull Family for Analyzing Bathtub Failure-Rate Data. *IEEE Transactions on Reliability* 1993; 42(2): 299–302, <https://doi.org/10.1109/24.229504>.
- Peng C Y. Inverse Gaussian Processes With Random Effects and Explanatory Variables for Degradation Data. *Technometrics* 2015; 57(1): 100–111, <https://doi.org/10.1080/00401706.2013.879077>.
- Peng W, Li Y F, Yang Y J et al. Inverse Gaussian process models for degradation analysis: A Bayesian perspective. *Reliability Engineering & System Safety* 2014; 130: 175–189, <https://doi.org/10.1016/J.RESS.2014.06.005>.
- Peng W, Li Y F, Yang Y J et al. Bayesian degradation analysis with inverse Gaussian process models under time-varying degradation rates. *IEEE Transactions on Reliability* 2017; 66(1): 84–96, <https://doi.org/10.1109/TR.2016.2635149>.
- Pourhassan M R, Raissi S, Hafezalkotob A. A simulation approach on reliability assessment of complex system subject to stochastic degradation and random shock. *Eksplatacja i Niezawodność – Maintenance and Reliability* 2020; 22(2): 370–379, <https://doi.org/10.17531/EIN.2020.2.20>.
- Quezada Del Villar A V, Rodríguez-Picón L A, Pérez-Olguín I J C, Méndez-González L C. Stochastic modelling of the temperature increase in metal stampings with multiple stress variables and random effects for reliability assessment. *Eksplatacja i Niezawodność – Maintenance and Reliability* 2019; 21(4): 654–661, <https://doi.org/10.17531/EIN.2019.4.15>.
- Rodríguez-Picón L A. Reliability assessment for systems with two performance characteristics based on gamma processes with marginal heterogeneous random effects. *Eksplatacja i Niezawodność – Maintenance and Reliability* 2017. doi:10.17531/ein.2017.1.2, <https://doi.org/10.17531/ein.2017.1.2>.
- Rodríguez-Picón L A, Rodríguez-Picón A P, Méndez-González L C et al. Degradation modeling based on gamma process models with random effects. *Communications in Statistics: Simulation and Computation* 2017. doi:10.1080/03610918.2017.1324981, <https://doi.org/10.1080/03610918.2017.1324981>.
- Romaniuk M. Optimization of maintenance costs of a pipeline for a V-shaped hazard rate of malfunction intensities. *Eksplatacja i Niezawodność - Maintenance and Reliability* 2017; 20(1): 46–56, <https://doi.org/10.17531/ein.2018.1.7>.

26. Romaniuk M, Hryniewicz O. Estimation of maintenance costs of a pipeline for a u-shaped hazard rate function in the imprecise setting. *Eksploatacja i Niezawodność – Maintenance and Reliability* 2020; 22(2): 352–362, <https://doi.org/10.17531/EIN.2020.2.18>.
27. SchÄbe H. Constructing lifetime distributions with bathtub shaped failure rate from DFR distributions. *Microelectronics Reliability* 1994; 34(9): 1501–1508, [https://doi.org/10.1016/0026-2714\(94\)90458-8](https://doi.org/10.1016/0026-2714(94)90458-8).
28. Si X S, Wang W, Hu C H et al. A Wiener-process-based degradation model with a recursive filter algorithm for remaining useful life estimation. *Mechanical Systems and Signal Processing* 2013; 35(1–2): 219–237, <https://doi.org/10.1016/j.ymssp.2012.08.016>.
29. Tang S, Guo X, Yu C et al. Accelerated degradation tests modeling based on the nonlinear wiener process with random effects. *Mathematical Problems in Engineering* 2014. doi:10.1155/2014/560726, <https://doi.org/10.1155/2014/560726>.
30. Tsai C-C, Tseng S-T, Balakrishnan N. Optimal Design for Degradation Tests Based on Gamma Processes With Random Effects. *IEEE Transactions on Reliability* 2012; 61(2): 604–613, <https://doi.org/10.1109/TR.2012.2194351>.
31. Wang H, Xu T, Mi Q. Lifetime prediction based on Gamma processes from accelerated degradation data. *Chinese Journal of Aeronautics* 2015; 28(1): 172–179, <https://doi.org/10.1016/j.cja.2014.12.015>.
32. Wang X. A pseudo-likelihood estimation method for nonhomogeneous gamma process model with random effects. *Statistica Sinica* 2008; 18: 1153–1163, <https://doi.org/10.2307/24308535>.
33. Wang X. Wiener processes with random effects for degradation data. *Journal of Multivariate Analysis* 2010; 101(2): 340–351, <https://doi.org/10.1016/J.JMVA.2008.12.007>.
34. Wang X, Xu D. An Inverse Gaussian Process Model for Degradation Data. *Technometrics* 2012; 52(2): 188–197, <https://doi.org/10.1198/TECH.2009.08197>.
35. Wu W F, Ni C C. A study of stochastic fatigue crack growth modeling through experimental data. *Probabilistic Engineering Mechanics* 2003; 18(2): 107–118, [https://doi.org/10.1016/S0266-8920\(02\)00053-X](https://doi.org/10.1016/S0266-8920(02)00053-X).
36. Xie M, Lai C D. Reliability analysis using an additive Weibull model with bathtub-shaped failure rate function. *Reliability Engineering & System Safety* 1996; 52(1): 87–93, [https://doi.org/10.1016/0951-8320\(95\)00149-2](https://doi.org/10.1016/0951-8320(95)00149-2).
37. Xie M, Tang Y, Goh T N. A modified Weibull extension with bathtub-shaped failure rate function. *Reliability Engineering & System Safety* 2002; 76(3): 279–285, [https://doi.org/10.1016/S0951-8320\(02\)00022-4](https://doi.org/10.1016/S0951-8320(02)00022-4).
38. Ye Z S, Chen N. The Inverse Gaussian Process as a Degradation Model. *Technometrics* 2014; 56(3): 302–311, <https://doi.org/10.1080/00401706.2013.830074>.
39. Zhang Z, Si X, Hu C, Lei Y. Degradation data analysis and remaining useful life estimation: A review on Wiener-process-based methods. *European Journal of Operational Research* 2018; 271(3): 775–796, <https://doi.org/10.1016/J.EJOR.2018.02.033>.
40. Zimmer W J, Keats J B, Wang F K. The Burr XII Distribution in Reliability Analysis. *Journal of Quality Technology* 2018; 30(4): 386–394, <https://doi.org/10.1080/00224065.1998.11979874>.
41. Zio E. Some challenges and opportunities in reliability engineering. *IEEE Transactions on Reliability* 2016; 65(4): 1769–1782, <https://doi.org/10.1109/TR.2016.2591504>.